C.P. No. 387
(18.084)
A.R.C. Technical Report

C.P. No. 387
(18.084)
A.R.C. Technical Report

MINISTRY OF SUPPLY

AERONAUTICAL RESEARCH COUNCIL

CURRENT PAPERS

HIGH REYNOLDS NUMBER TESTS ON A 70° L.E. SWEEPBACK DELTA WING AND BODY (H.P. 100) IN THE COMPRESSED AIR TUNNEL

By

R. W. F. Gould, B.Sc., A.F.R.Ae.S., and C. F. Cowdrey, B.Sc.,

of the Aerodynamics Division, N.P.L.

LONDON . HER MAJESTY'S STATIONERY OFFICE

1958

PRICE 3s 6d NET

High Reynolds Number Tests on a 70° L.E. Sweepback Delta Wing and Body (H.P. 100) in the Compressed Air Tunnel

- By -
R. W. F. Gould, B.Sc., A.F.R.Ae.S., and C. F. Cowdrey, B.Sc.,
of the Aerodynamics Division, N.P.L.

December, 1955

SUMMARY

Values of lift, drag and pitching moment coefficients are given for a model of the H.P. 100 delta wing with sharp leading edges and with a body attached, over a range of Reynolds numbers from 1×10^6 to 12×10^6 and at incidences up to 42°. Photographs of the traces of an oil/titanium oxide mixture, on the surface, indicating flow directions, are included. The results show no appreciable scale effect.

Introduction

A larger model of the H.P. 100 wing, with a suitable body attached, had already been tested to a Reynolds number of 0.9×10^6 in the Handley Page wind tunnel. Similar tests to a high Reynolds number were made in the Compressed Air Tunnel with corresponding visual tests, in an attempt to link any scale effects with flow patterns. The incidence range covered was 45° starting from a small negative value.

The Model

The wing plan was a delta with 70° leading edge sweepback. The section was biconvex, generated by circular arcs and having a maximum thickness of 4% of the local chord. The wing was set along the centre-line of a body of fineness ratio 20.7 as shown in Fig. 1.

Considerations of tunnel blockage at the highest incidence and of the wind forces on the model led to the span being limited to 18". The maximum lift and drag forces experienced were 300 lb and 360 lb respectively.

The wing was formed of selected plywood bonded to a substantial steel core and phenoglazed. The body was of wooden construction.

The Need for Special Support Arrangements

Models in the Compressed Air Tunnel are generally supported from above, by two streamlined rods, pin jointed to the wings, with a third streamlined rod, pin jointed to the fuselage, farther astern. The third rod can be driven up and down for change of incidence and its position relative to the main support is largely determined by the incidence range to be covered. In most models the front supports can be placed in regions of substantial wing thickness, at the same time positioning the rear rod so that it never comes under compression (which would lead to incidence changes from buckling of the rod). In the case of the H.P. 100 model it was clear that the wing was too thin to permit adequately spaced front supports and, in any case, the severe sweepback would have placed these supports so far astern that buckling of the rear support would have been inevitable. Moreover such make-shift expedients as were possible to overcome this difficulty would have resulted in undesirably large wing/support interference and this would have thrown doubt on any conclusions drawn from the work.

The/

Published with permission of the Director, National Physical Laboratory, and of Handley Page, Limited.

The Support Arrangement Used

The support arrangement devised is shown in Fig. 2. A pair of overhead front members, attached to the balance and similar to those normally used, though shorter, supported a horizontal beam, into the centre of which a sweptback strut was fixed. An inclined tie bar, from the centre of the beam direct to the balance framework, took most of the resultant loading on the strut. This reduced the displacement of the model under load to reasonable proportions, with a corresponding reduction in the magnitude of the corrections from this cause. The design problem was then reduced largely to one of ensuring that the pins anchoring the beam at each end, and those holding the strut to the beam could withstand the shear forces arising from the torsion loads on the beam. There remained stringent requirements of manufacture, particularly in fitting these pins, so that no backlash was present.

The rigidity in yaw and roll common to the normal three point suspension having been removed, adequate compensation was obtained by making the lower end of the strut in the form of a flat tongue of substantial surface area, fitting closely into a slot machined in the central steel core of the model. The cheeks of the tongue were of phosphor bronze. Initially a steel to steel bearing had seized up, probably due to molecular adhesion between the similar faces. Graphite grease was used as a lubricant and the modified bearing behaved perfectly.

The support gear was well shielded from the wind with stream-lined guards down to the level indicated in Fig. 2.

Displacement of Model

In assembling the support gear it is possible to arrange for the axis of the main bearing support to coincide with the pitching moment axis of the balance. If, on loading in a wind, the model position changes, it is necessary to correct the balance moment readings to the new position of the model bearing and also to correct the incidence in the light of the relative movements of the bearing axes of the front and rear supports. The rear support rod will swing in an arc struck from its upper pivot, as compelled by the fixed spacing between the two bearings in the model.

The loading also causes a swing of the model in an arc centred roughly in the horizontal beam so that lift and drag loadings each produce both horizontal and vertical deflections at the front support bearing.

On this account, horizontal and vertical loadings were applied, in turn, to the front support strut at the bearing position and dial gauges were used to measure the resulting horizontal and vertical deflections.

As would be expected, it was found that combined horizontal and vertical loads produced deflections which were simple additions of those obtained by separate horizontal and vertical loading.

The standard of craftsmanship in the manufacture and fitting of the model and support gear was excellent and as a result only negligible backlash was encountered on loading and unloading the support. Thus in spite of appreciable deflections in actual running conditions, corrections for these deflections were applied with confidence. The maximum shifts encountered under running conditions amounted to almost 0.2 in. horizontally and 0.05 in. vertically, which resulted in a maximum correction on Cm of nearly 0.07 and on incidence of 0.7°.

Initial/

Initial Difficulties

During the first few tests the main support bearing gave trouble, as mentioned earlier, and eventually jammed altogether. This prolonged the running time and although the wing tips had started as paper-thin points, by the time the highest Reynolds number tests were attempted, one of the tips had slightly deteriorated and a severe oscillation developed near the stall. It is probable that the slight asymmetry between the wing tips gave rise to phase and magnitude changes between the vortices from each wing and the resulting instantaneous forces might well have produced rolling and yawing moments large enough to account for the oscillation experienced. The intact wing tip was trimmed with a pair of scissors to correspond with the damage tip and although the oscillation was greatly reduced, it was still not possible to proceed to the highest incidence at the highest R.N.

A slight reduction of R enabled a satisfactory run to be completed and, in view of the insignificant scale effect between any results obtained up to that stage, it was not considered necessary to repair the wing tips in order to complete the highest run.

Pitching Moment Axes

The tests in the Handley Page wind tunnel were undertaken with reference to a pitching moment axis on the model centreline and $0.8403\ \bar{c}$ from the trailing edge, the position being shown in Fig. 1 as the specified centre of gravity line. In the present tests compression in the rear support could only be avoided by using a primary pitching moment axis further upstream, on the centreline but $1.0305\ \bar{c}$ from the trailing edge. In addition to presenting results relative to this latter axis, moments have also been converted to the preferred axis.

Results

Table 1 shows the values of the various coefficients obtained in the tests at four Reynolds numbers, from 1×10^6 to 12×10^6, undertaken at pressures of 2 to 25 atmospheres approximately. The incidence and moment coefficient values have been corrected for the displacement of the model under load as mentioned earlier. An estimate was made of the drag of the exposed portion of the front support, (that of the rear support rod being known). The total correction was small and was used in computing the values of C_D. No attempt was made to measure the interference between the supports and body, since the provision of a dummy model would have taken too long and, in any case, only comparative results were called for. The values of C_L and C_m at zero incidence show that the interference was small and qualitatively as expected - the loss of pressure behind the supports producing a small negative lift and positive pitching moment - it being remembered that positive lift acts downwards in the Compressed Air Tunnel.

The Graphs

The results are plotted in Figs. 3 to 8. It will be seen that scale effects on C_L and C_D nowhere exceed 2.5% of the maximum values, and are generally much less, the effect on C_m being correspondingly small. There is a marked concavity in the curve of lift against incidence, (Fig. 3), over the working range up to a point of inflexion at about 23°, ($C_L \approx 1.0$), and $C_{L_{max.}}$ would appear to be about 1.26.

This concavity, (increase of slope with increasing incidence) has been accounted for theoretically, in terms of the part span vortex sheets, by Küchemann (Ref. 1). With very highly swept wings, the vortex sheets exist from the lowest incidences and continually increasing

extra/

extra lift, on this account, is evident over most of the working range. In less swept wings, the part-span vortex sheets develop and begin to move inboard at an appreciable incidence and the concavity of the lift curve only appears above this value.

Fig. 4 is the graph of C_D against α and emphasizes the large values of C_D obtained at the higher incidences. In Fig. 5, C_D has been plotted against $C_L{}^2$, and despite the fact that a small part of the lift and drag is due to the body, the range of incidence over which C_D varies linearly with $C_L{}^2$ is noteworthy. Departure from linearity of this graph also occurs at about 23°, the incidence at which the point of inflexion appeared on the lift curve.

Fig. 6 shows the variation of Cm with α by direct measurement using the arbitrary pitch axis of the model, and Fig. 7 shows the curve computed for the preferred axis through the specified centre of gravity. The completely different character of these two graphs for a modest change of axis position means that only where sudden changes of moment occur on both curves for the same incidence can a radical change of flow pattern be expected.

In Fig. 6 $dCm/d\alpha$ is highly negative over the major working range (largely due to the moment axis chosen), whereas in Fig. 7 there is a change from a slightly negative value of $dCm/d\alpha$ below about 10° to a large positive value from 10° to the stall. In Fig. 6 the departure from linearity near 25° corresponds with a pronounced reduction in the lift slope in Fig. 3, but at the same incidence in Fig. 7, either there is no corresponding feature, or else it is masked by the general steepness of the curve in that region. Also, the sudden change of slope in Fig. 7 at about 9° does not appear in Fig. 6. This rapid change of slope (referred to the specified centre of gravity) would seem to be due to the summation of separate small effects of lift and drag and not from a drastic change in the flow pattern at this incidence. Fig. 8 shows the corresponding graph of Cm against C_L.

Comparison with Previous Results

Ref. 2 includes graphs of tests in the Handley Page wind-tunnel, of 7 ft × 5 ft closed working section (compared with the 6 ft circular open jet C.A.T. section), on a model which was larger than that used in the C.A.T. tests. Up to about 20° the C.A.T. and Handley Page curves are very similar in character, but at higher incidences the latter results show lift coefficients up to 20% higher than those given in this report. This difference might be attributable to a blockage effect at high incidences in the Handley Page tests.

Flow Visualisation

In their tests (Ref. 2), Messrs. Handley Page used an oil/titanium oxide mixture for surface flow visual tests. To help interpret these surface patterns, they also set up a lattice of wires carrying streamers above the model in the tunnel. A simplified sketch of the flow patterns in the outboard region as shown by the streamers, is compared with the corresponding typical surface flow pattern in Fig. 9. The shortcomings of these surface flow patterns as clues to the complete flow pattern are obvious.

Inadequate viewing facilities for studying streamers inside the Compressed Air Tunnel at pressure, precluded the convenient extension of this type of test to high Reynolds numbers and only the oil surface flow patterns were recorded, at Reynolds numbers of 2 × 10⁶ and 5 × 10⁶, and at angles up to the stall. Earlier, wool tufts had been stuck at suitable stations on the wing for observations at atmospheric pressure. It was

soon/

soon obvious that the flow directions indicated were influenced by the presence of the tufts and these observations were abandoned. In removing these tufts, the discoloration of the surface by the acetate base adhesive became noticeable and these blemishes on the photographs reproduced in this report should be discounted as the surface was in fact everywhere quite smooth.

The Oil Technique

The oil mixture used for Reynolds numbers in the 1×10^6 to 6×10^6 range was the same as that normally used in atmospheric pressure tunnels. Titanium oxide powder was moistened with a few drops of diesel oil, then a few drops of oleic acid were added with thorough mixing to disperse the lumps. Finally more diesel oil was added and the mixture stirred until the required consistency was obtained. Depending on the Reynolds number and incidence of the test in hand, the consistency of the mixture used had to be varied to permit flow due to the shear forces without undue flow under gravity. For tests at $R < 1 \times 10^6$ improved flow was found with a mixture in which the diesel oil was replaced by ordinary paraffin. Since these tests, replacement of the diesel oil with one of the commercial detergent oils and some fractionated paraffin has given excellent flow pictures at even higher Reynolds numbers. The amount and particular fraction of paraffin depends on the pressure and Reynolds number of the test. The aim should be for the paraffin to evaporate in a reasonable running time leaving the mixture viscous enough to prevent flow under gravity. The mixture was applied with the wing surface horizontal, and then air was admitted to the tunnel from reservoir bottles, the wing set at incidence, the tunnel speed attained quickly and maintained for a suitable time. After stopping the tunnel, the incidence was reset to zero and the tunnel exhausted for inspection.

Photography

The copying technique of photography was employed in which two photofloods are used, each at 45° to the span line and in a plane normal to the centre-line of the model, with the camera halfway between the lamps. When the lamps and camera were ready for use the wing was set to a pre-determined incidence, just normal to the camera line of view. L. P. K. Hillman, A.R.P.S., of the Central Photographic Section, N.P.L., took the photographs. Copies of some of these are included at the end of the report.

The Photographs

A photograph taken at 1.1° incidence showed surface flow everywhere parallel to the model axis and has therefore not been included. Leading edge separation begins very early and is well defined by 4° (Plate 1). The most noticeable feature of the photographs reproduced is the inboard spread of the influence of the main rolled-up vortex sheets as incidence is increased to the stalling angle. This can be seen from the movement of the stagnation line (Fig. 9) and by regarding the flow direction at the trailing edge in the plates. By the time the stalling angle has been reached the region of influence of these vortices appears to have covered the whole wing. There seems to be no conspicuous change of surface flow associated with the reversals in the C_m curves (Figs. 6, 7 and 8).

Conclusion

The tests confirmed the expectation that there would be no appreciable scale effect on the force and moment coefficients over the range of Reynolds numbers 1×10^6 to 12×10^6. The surface

flow/

flow patterns follow the changes generally associated with highly swept wings and do not reveal any sudden changes with incidence likely to account for the particular shape of the pitching moment curves shown in Figs. 6, 7 and 8.

Acknowledgements

The authors wish to acknowledge the assistance of K. T. Wright of Handley Page, Ltd., and C. A. Culverhouse of Aerodynamics Division, N.P.L., who co-operated in the design of the support gear, which was largely constructed in the Handley Page workshop and finished and assembled by H. F. Lovesey of Aerodynamics Division, N.P.L. M. D. Timothy assisted in the observations and the authors wish to record that valuable advice was given by C. Salter throughout the tests.

References

Nos.	Author(s)	Title, etc.
1	Küchemann, D.	A simple method for calculating the span and chordwise loading on straight and swept wings of any given aspect ratio at subsonic speeds. To be R. & M. 2935. August, 1952.
2	Lee, G. H. (Handley Page, Ltd.)	Note on the flow around delta wings with sharp leading edges. R. & M. 3070. September, 1955.

TABLE 1/

TABLE 1

H.P.100 C.A.T. Test Results

P = 25.2 ATMOS
ρV^2 = 367.0 lb/sq ft
V = 79.8 f.p.s.
R = 12.22×10^6

α	C_L	C_D	C_M	$C_M(C.G)$
-3.0	-0.102	0.0098	0.0286	0.0091
-1.6	-0.056	0.0062	0.0178	0.0072
+1.15	+0.022	0.0043	-0.0014	00.0028
3.85	0.111	0.0092	-0.0218	-0.0007
6.5	0.212	0.0231	-0.0431	-0.0026
9.1	0.315	0.0485	-0.0650	-0.0044
11.7	0.428	0.0834	-0.0858	-0.0029
14.5	0.547	0.131	-0.1065	+0.0004
16.8	0.668	0.192	-0.1275	0.0048
19.35	0.790	0.262	-0.1471	0.0115
21.9	0.909	0.348	-0.1651	0.0201
24.45	1.020	0.445	-0.1822	0.0299
27.0	1.122	0.536	-0.1916	0.0463
29.6	1.193	0.660	-0.1944	0.0648
32.25	1.236	0.753	-0.2057	0.0705

P = 23.85 ATMOS
ρV^2 = 312.2 lb/sq ft
V = 75.2 f.p.s.
R = 10.85×10^6

α	C_L	C_D	C_M	$C_M(C.G)$
-3.0	-0.098	0.0098	0.0283	0.0092
11.7	0.438	0.0825	-0.0867	-0.0019
21.95	0.924	0.354	-0.1685	0.0199
29.7	1.202	0.647	-0.1962	0.0645
32.3	1.248	0.757	-0.2077	0.0706
33.65	1.256	0.804	-0.2137	0.0714
35.0	1.256	0.843	-0.2165	0.0731
36.35	1.229	0.876	-0.2108	0.0770
37.75	1.197	0.902	-0.2107	0.0754
41.9	1.083	0.946	-0.2185	0.0562

P = 4.65 ATMOS
ρV^2 = 63.4 lb/sq ft
V = 76.4 f.p.s.
R = 2.25×10^6

α	C_L	C_D	C_M	$C_M(C.G)$
-3.0	-0.101	0.0108	0.0274	0.0083
11.8	0.434	0.0873	-0.0894	-0.0051
22.1	0.926	0.358	-0.1699	0.0193
29.9	1.216	0.668	-0.2138	0.0506
31.25	1.226	0.719	-0.2085	0.0625
32.6	1.244	0.767	-0.2135	0.0654
33.95	1.255	0.812	-0.2155	0.0706
35.35	1.237	0.845	-0.2158	0.0706
36.75	1.205	0.868	-0.2125	0.0707
38.15	1.200	0.909	-0.2172	0.0709
42.4	1.055	0.938	-0.2385	0.0298

P = 1.91 ATMOS
ρV^2 = 25.0 lb/sq ft
V = 74.6 f.p.s.
R = 0.924×10^6

α	C_L	C_D	C_M	$C_M(C.G)$
-3.0	-0.103	0.0125	0.0289	0.0092
-1.6	-0.060	0.0093	0.0180	0.0065
1.15	+0.020	0.0071	-0.0021	0.0017
3.85	0.111	0.0138	-0.0231	-0.0018
6.5	0.215	0.0272	-0.0447	-0.0035
9.15	0.327	0.0557	-0.0694	-0.0063
11.75	0.443	0.0936	-0.0907	-0.0045
14.4	0.562	0.143	-0.1128	-0.0025
16.95	0.681	0.200	-0.1302	+0.0050
19.55	0.805	0.271	-0.1505	0.0113
22.1	0.923	0.361	-0.1704	0.0186
24.7	1.050	0.458	-0.1889	0.0295
26.0	1.110	0.511	-0.1947	0.0383
27.3	1.153	0.564	-0.1972	0.0473
28.6	1.190	0.624	-0.2068	0.0490
29.95	1.225	0.676	-0.2184	0.0483
31.3	1.250	0.726	-0.2222	0.0537
32.65	1.255	0.770	-0.2167	0.0640
34.0	1.268	0.814	-0.2208	0.0668
35.4	1.242	0.837	-0.2152	0.0711
36.75	1.221	0.861	-0.2178	0.0676
38.2	1.188	0.898	-0.2187	0.0655
42.45	1.046	0.923	-0.2462	0.0201

18,084.
FIG 1

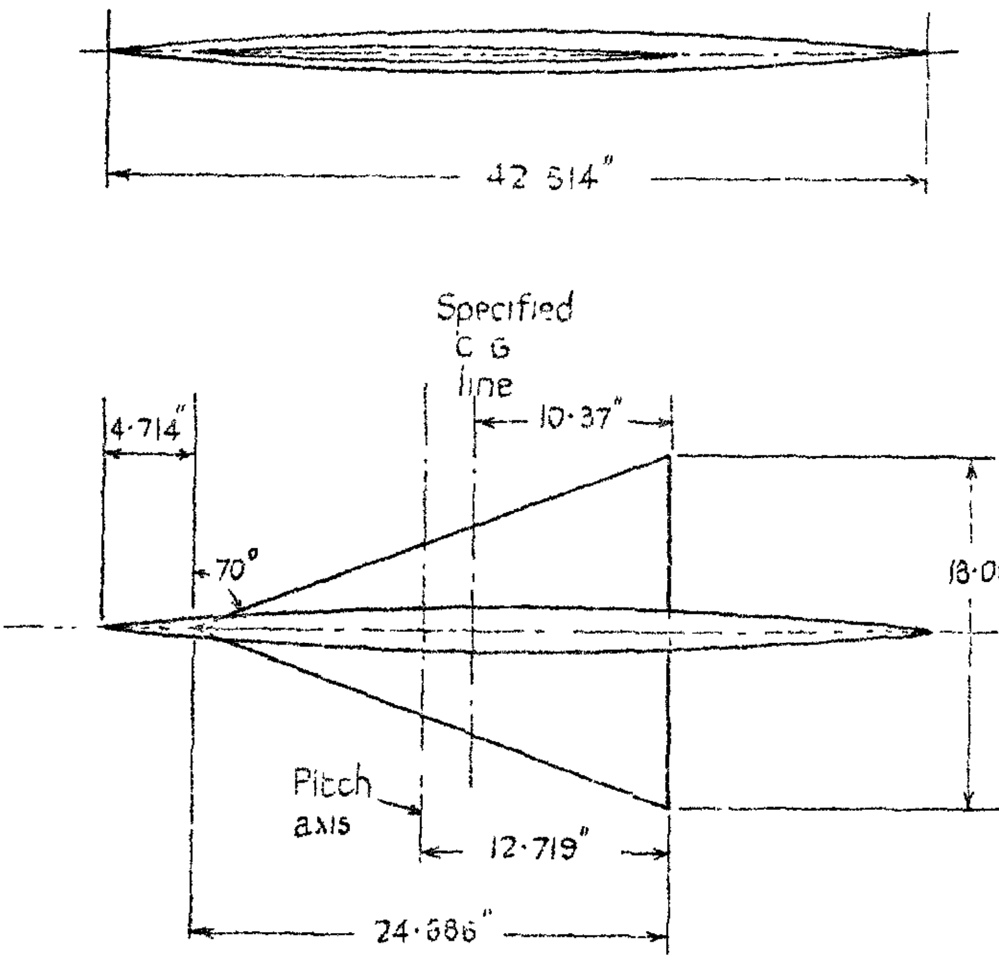

Wing t/c	= 4% (max thickness 0·988")
Wing area	= 1·543 sq.ft
Wing section	= circular arcs
Fuselage cross section	= circular
Fuselage max dia.	= 2 057"
Standard mean chord $\bar{c}$	= 1·028 ft

Pitching moment axis on ℄ 1·0305 $\bar{c}$ from T E.
Nominal C G on ℄ 0·8403 $\bar{c}$ from T E.

$\frac{1}{35}$ scale H P 100 wing and body model

DT

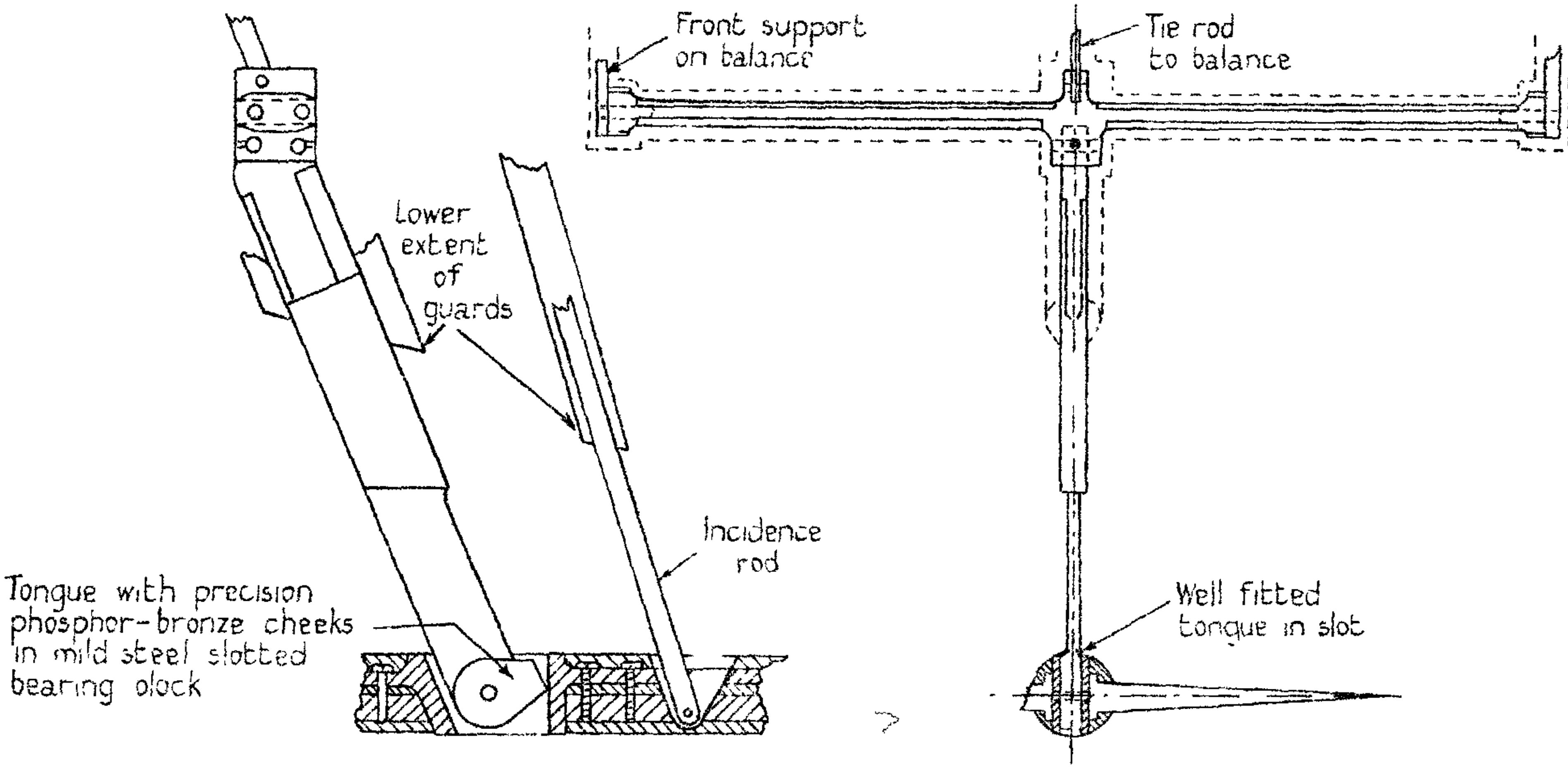

Tandem support arrangements for H P 100

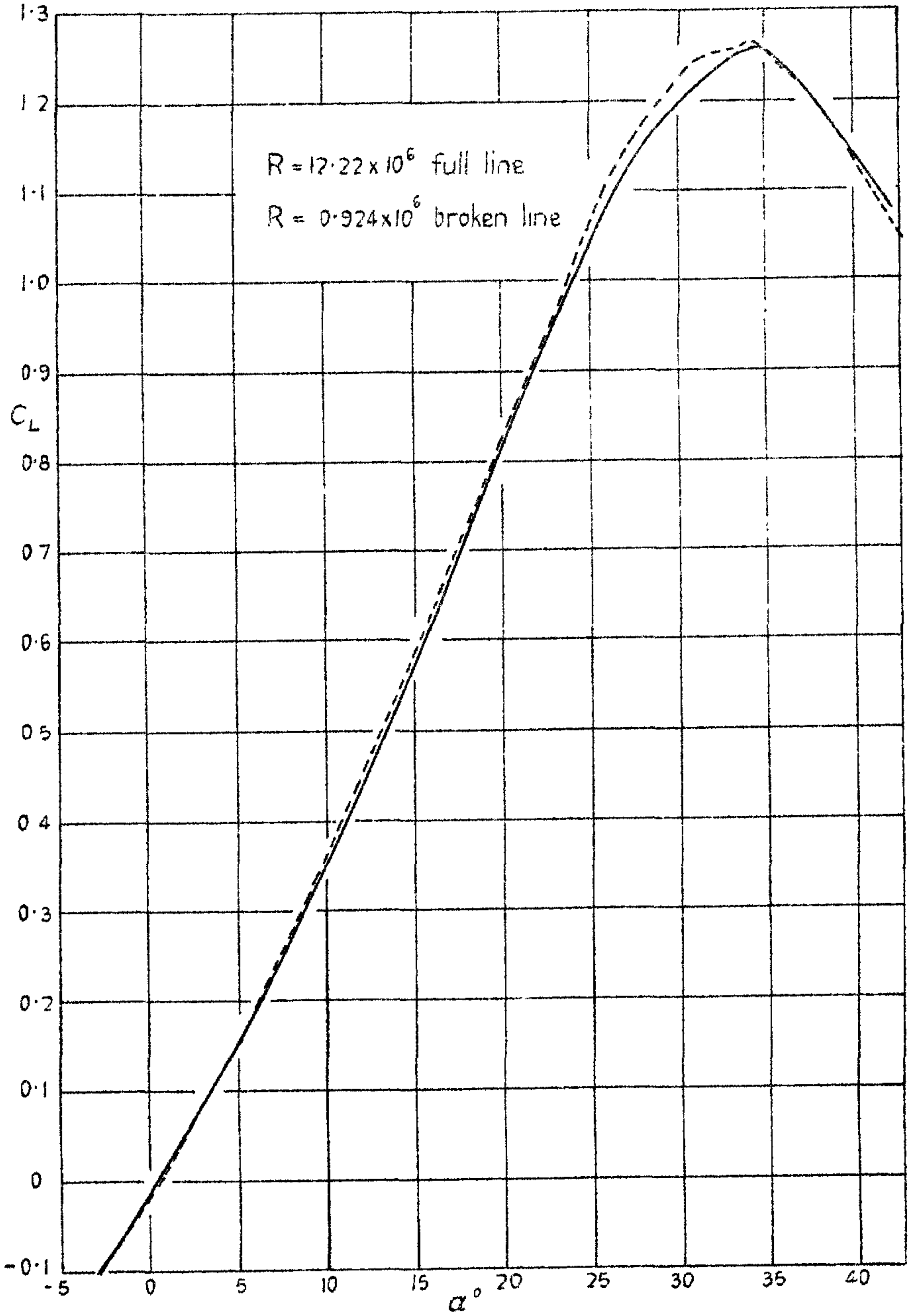

C_L for H P 100 wing and body plotted against α

18,084
FIG 4

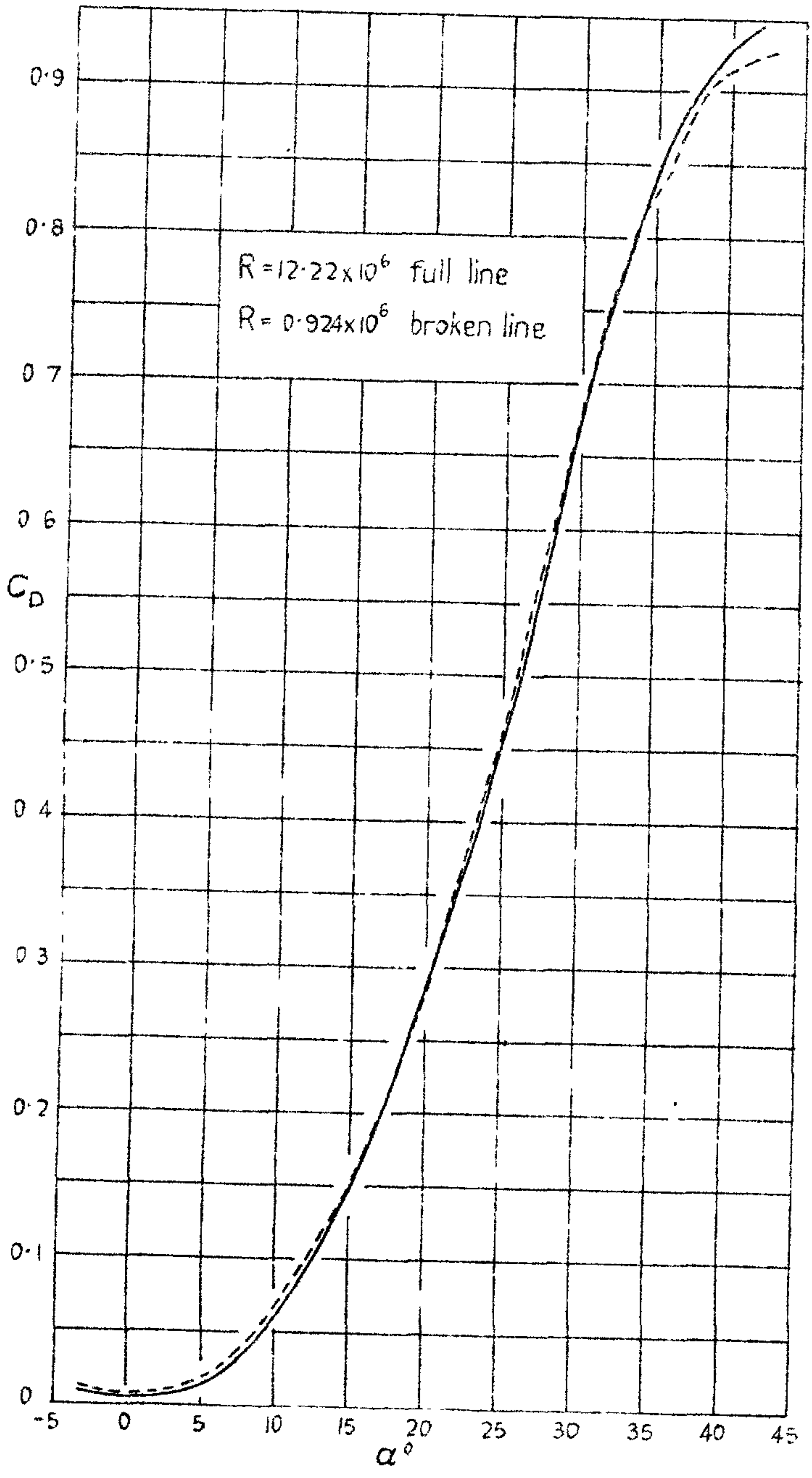

C_D for H P 100 wing and body plotted against α.

18,084

FIG. 5.

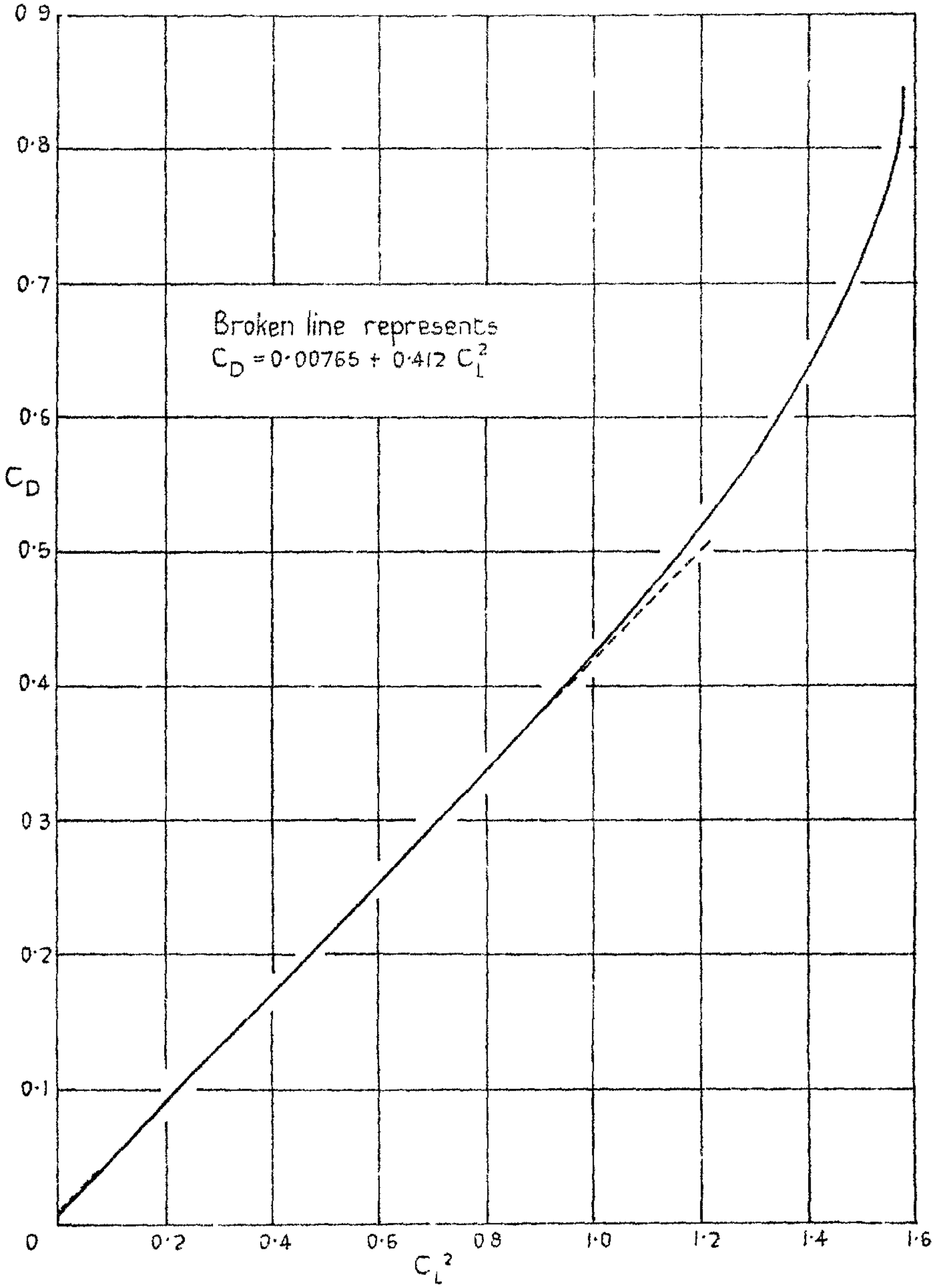

C_D for H.P. 100 wing and body plotted against C_L^2

D.T.

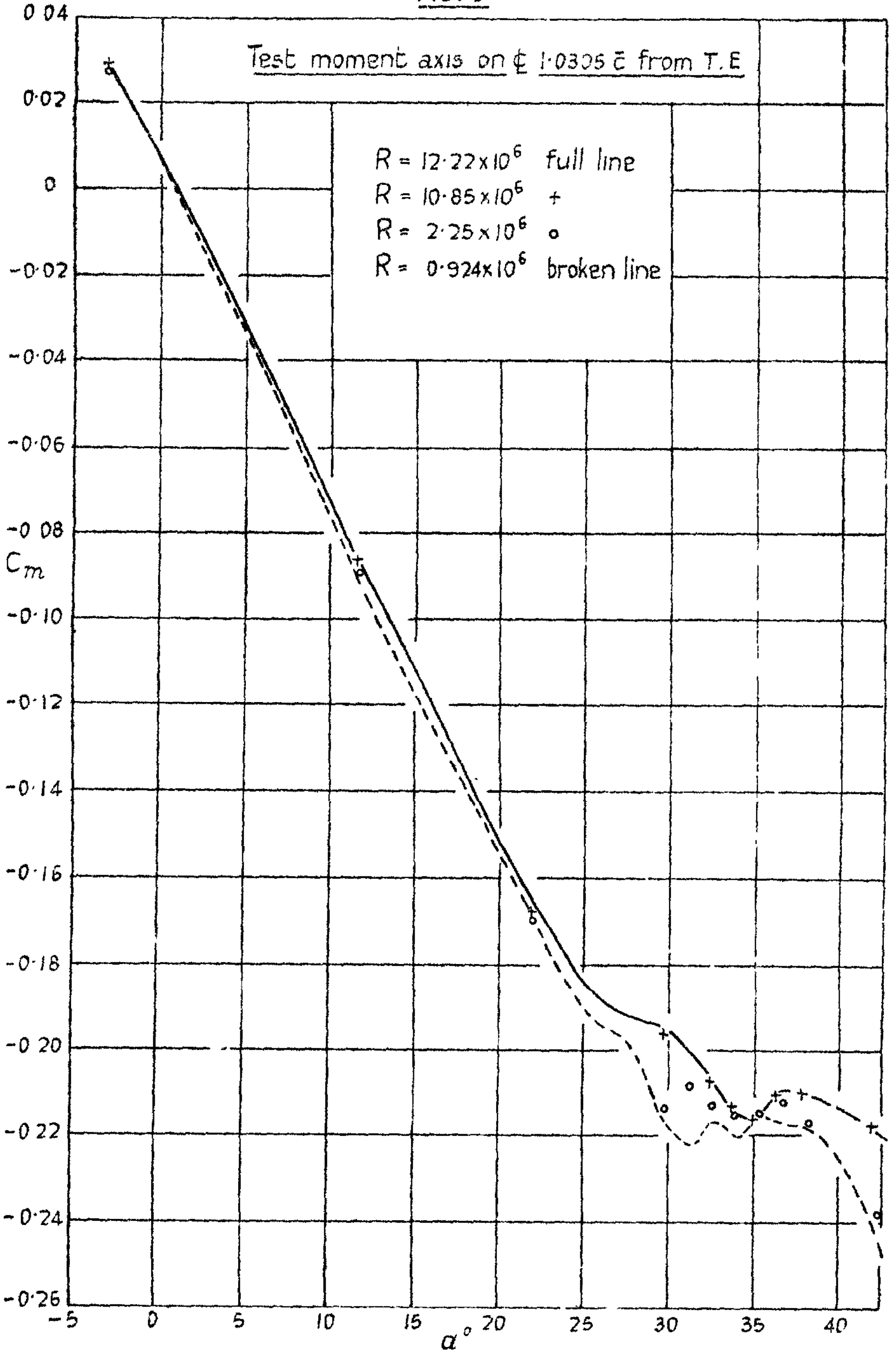

C_m for H.P. 100 wing and body plotted against α

Specified C G on ℄ 0 8403c̄ from T E

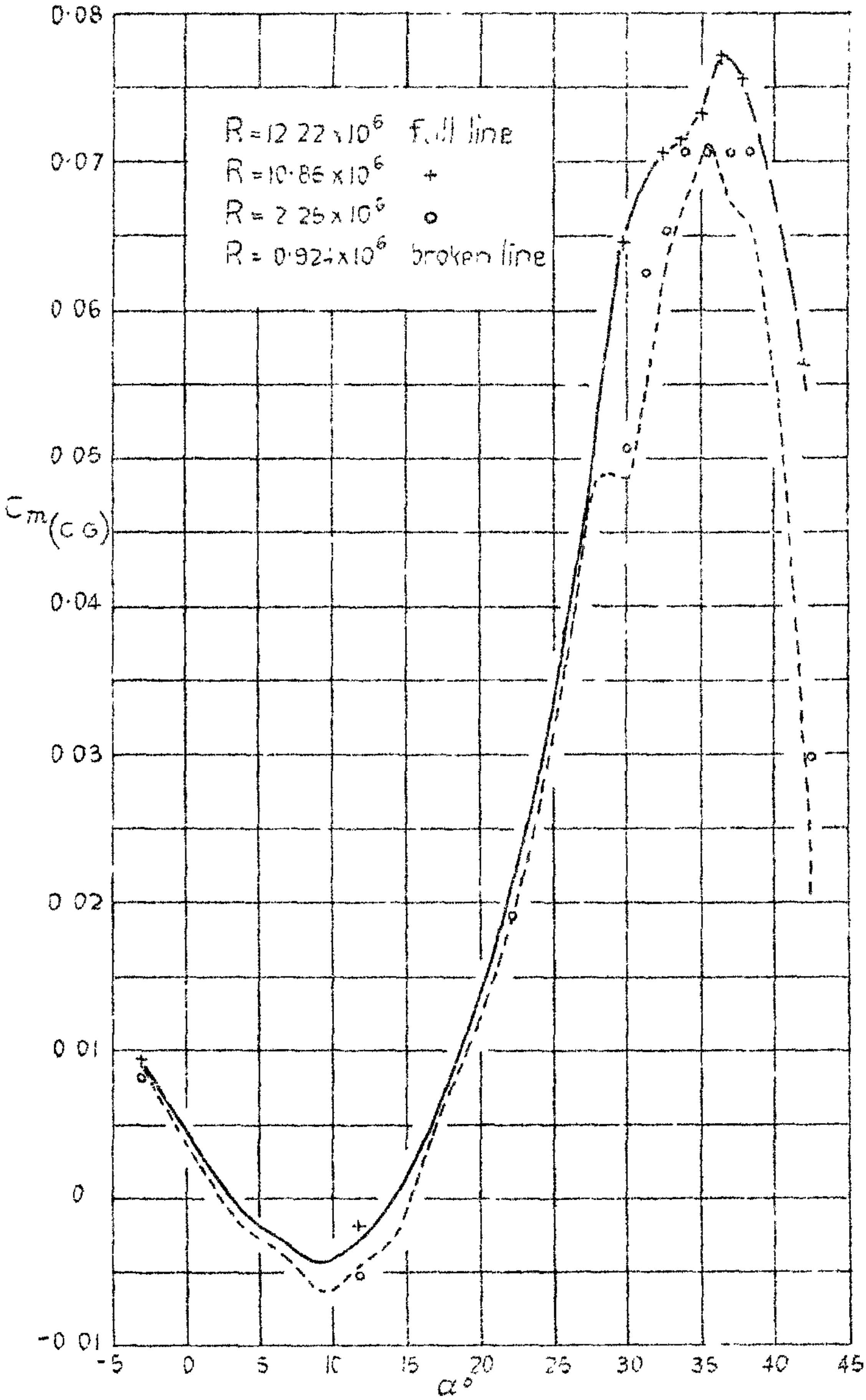

C_m about specified centre of gravity for H P 100 wing and body against α

18,084
FIG 8.

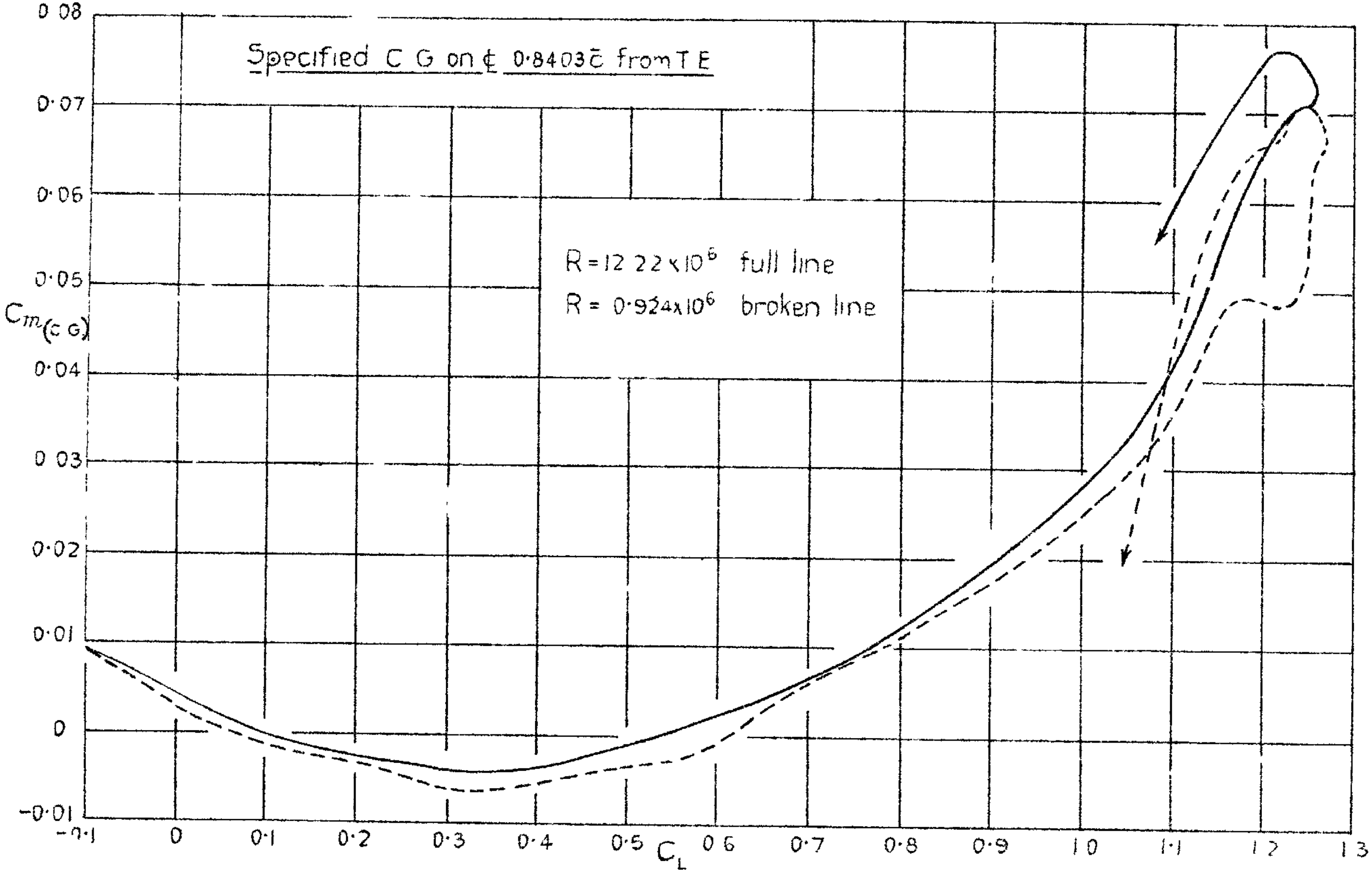

C_m referred to specified C G. position for H P 100 wing and body against C_L

18,084
Fig. 9.

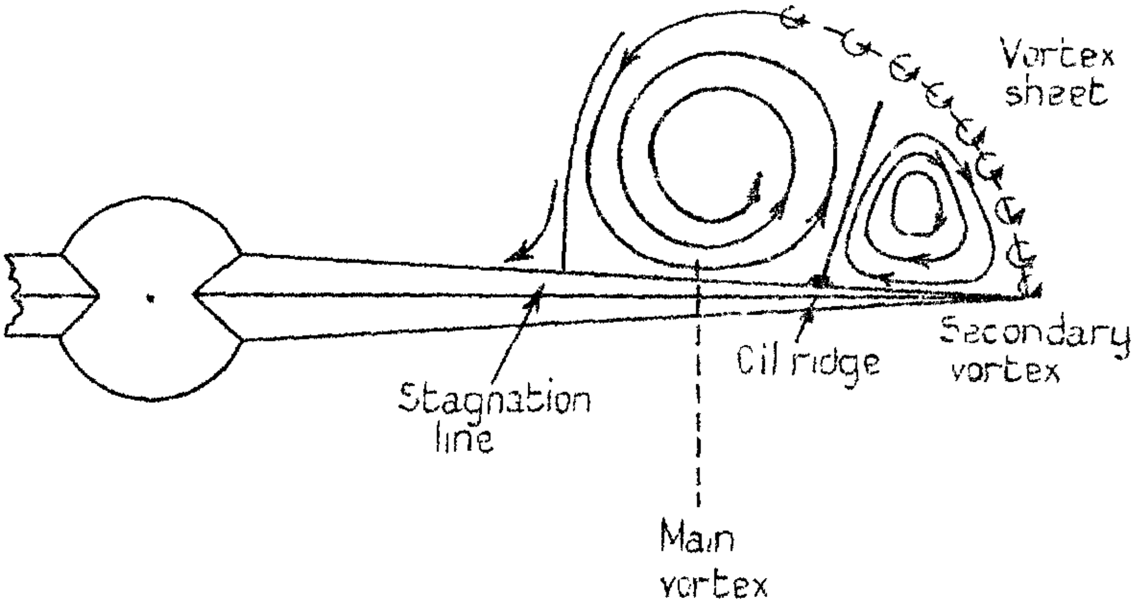

Typical rear view of tip flow pattern

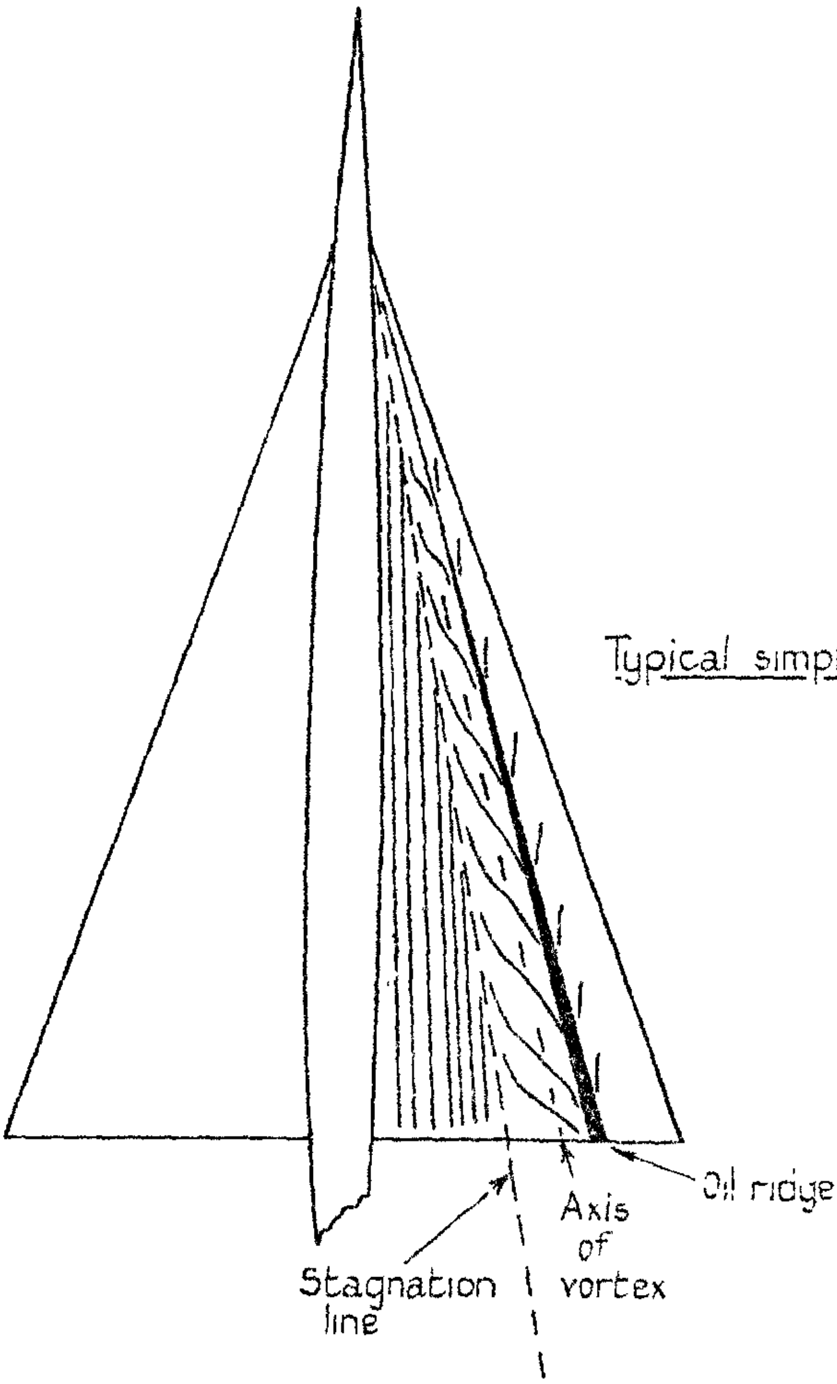

Typical simplified oil picture

D T

Plate I.

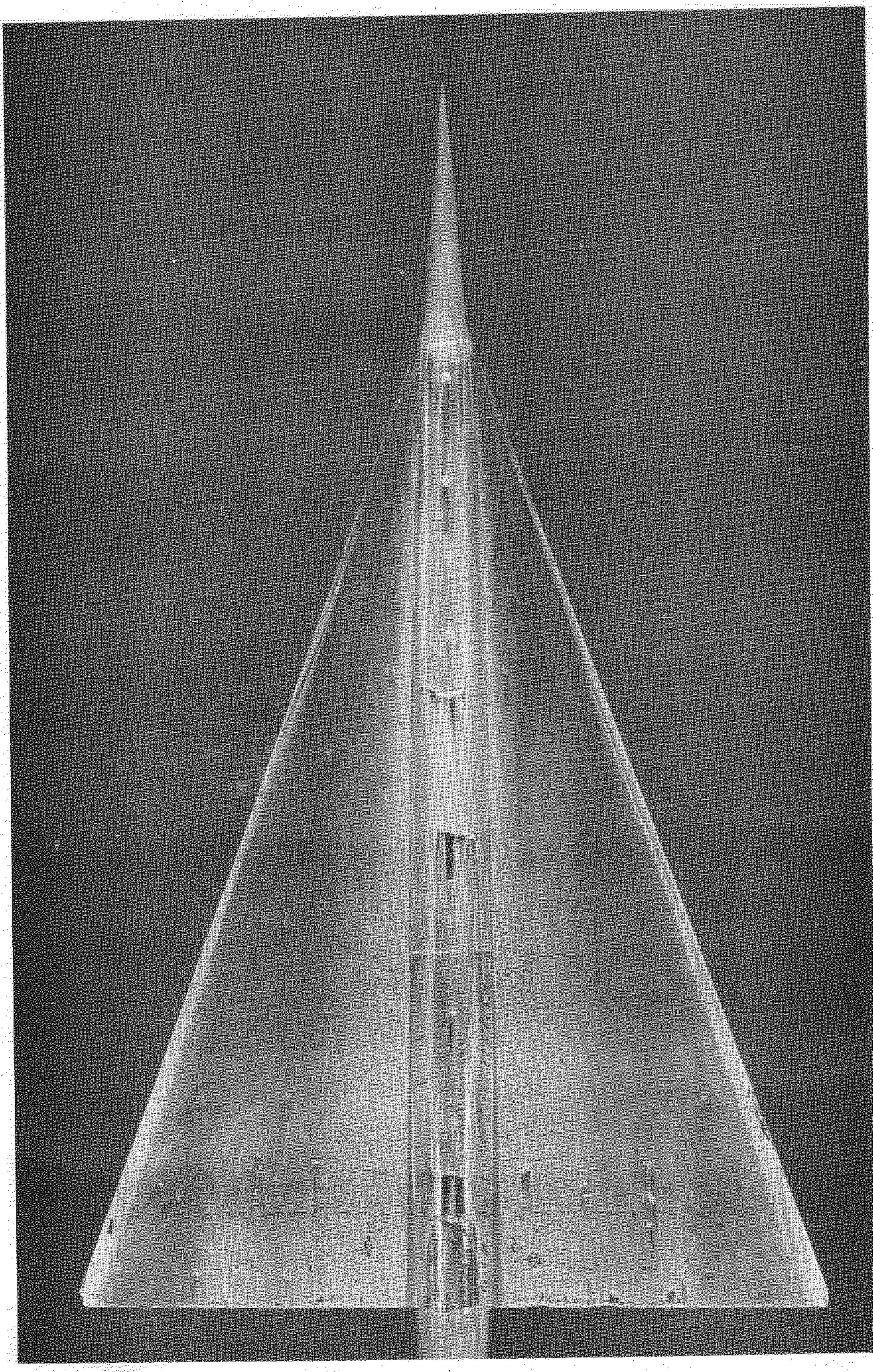

$\alpha = 3 \cdot 9^{0}$ $R = 5 \cdot 6 \times 10^{6}$

H.P. 100

Plate 2.

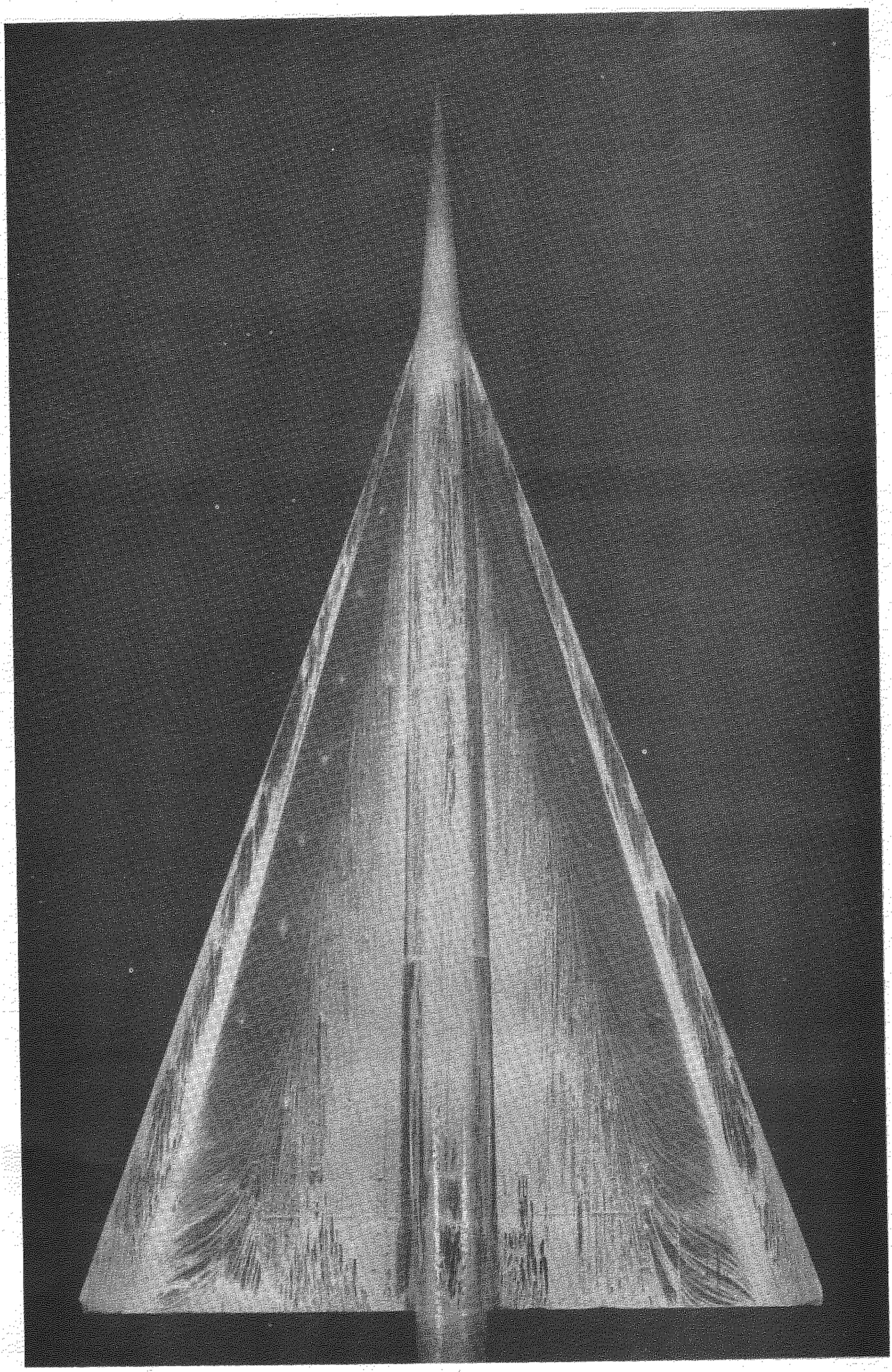

$\alpha = 9{\cdot}3^{0}$ $R = 2{\cdot}2 \times 10^{6}$

H.P. 100

Plate 3.

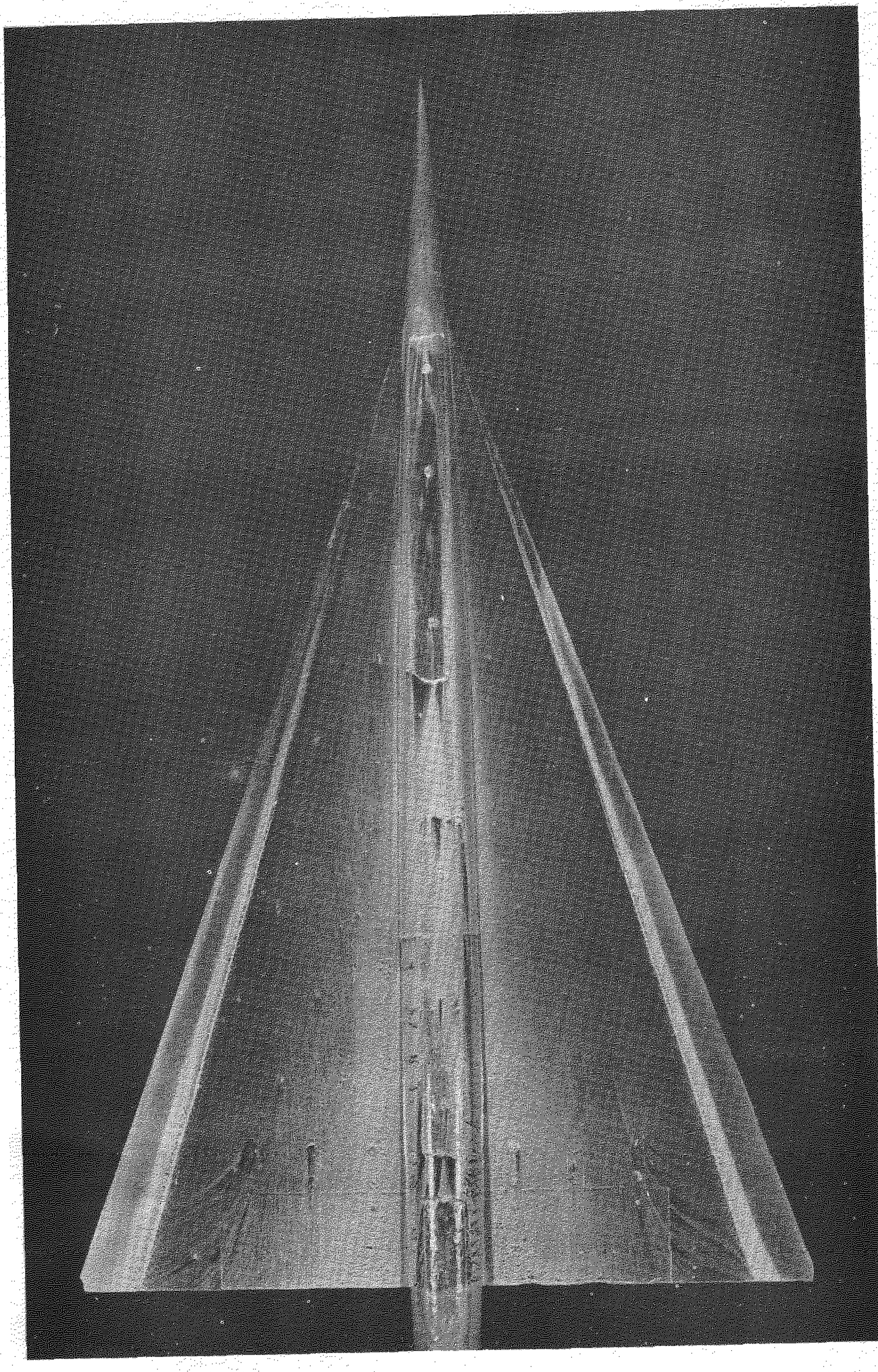

$\alpha = 9{\cdot}3^{\circ}$ $R = 5{\cdot}2 \times 10^{6}$

H.P. 100

Plate 4.

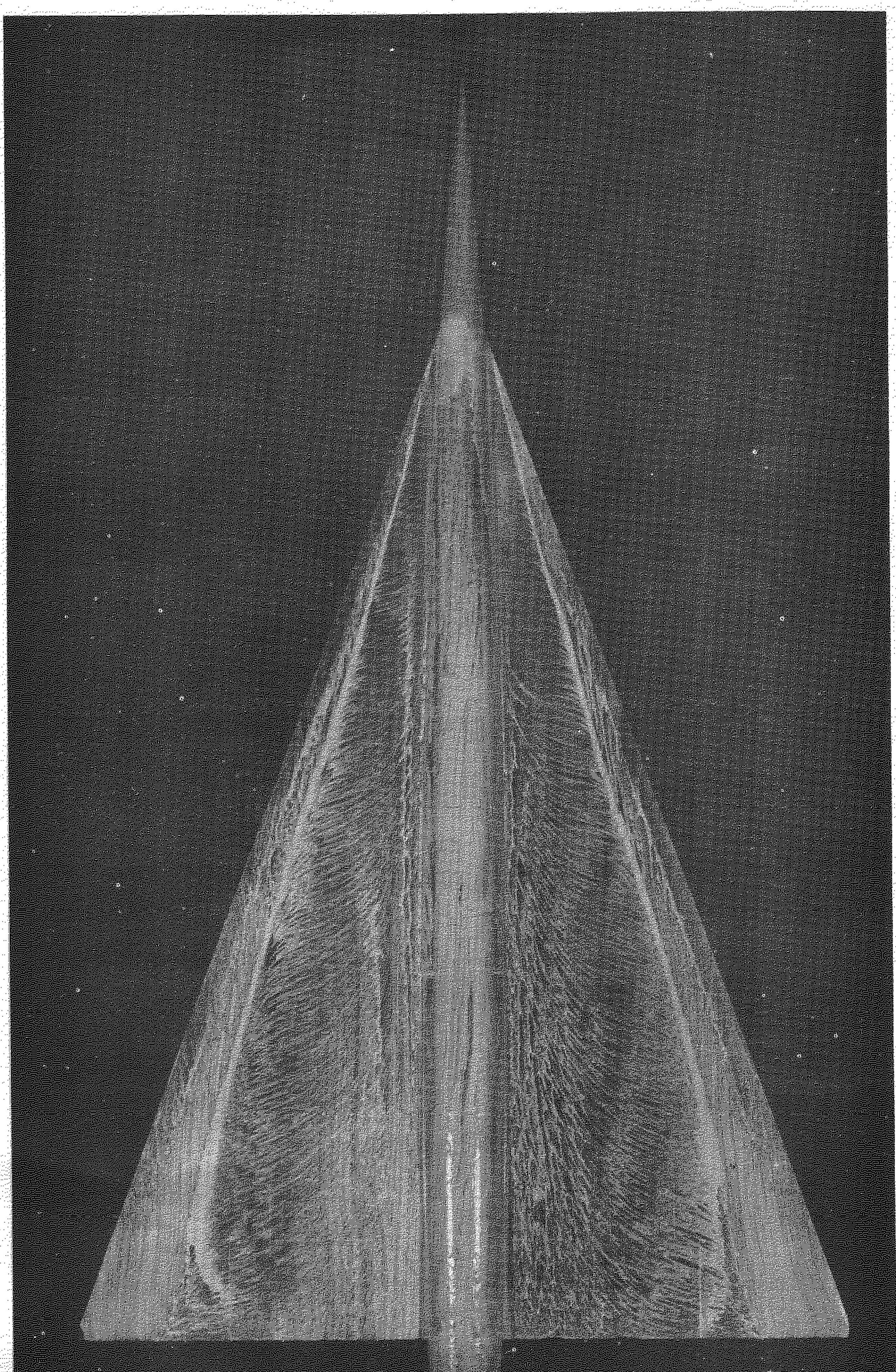

$\alpha = 23{\cdot}8^{\circ}$ $R = 0{\cdot}49 \times 10^{6}$

H.P. 100

Plate 5.

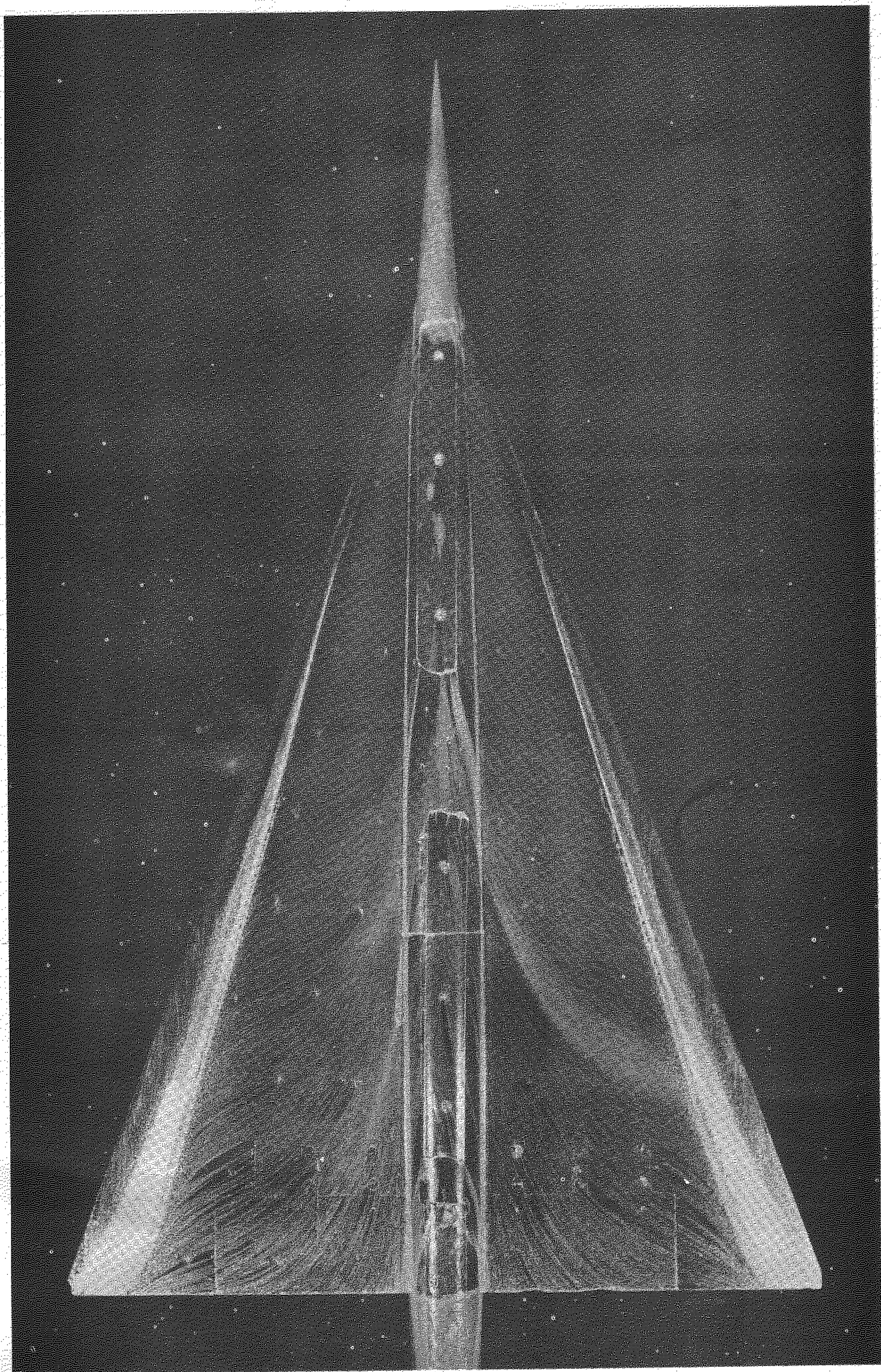

$\alpha = 23 \cdot 8^{\circ}$ $R = 5 \cdot 5 \times 10^{6}$

H.P. 100

Plate 6.

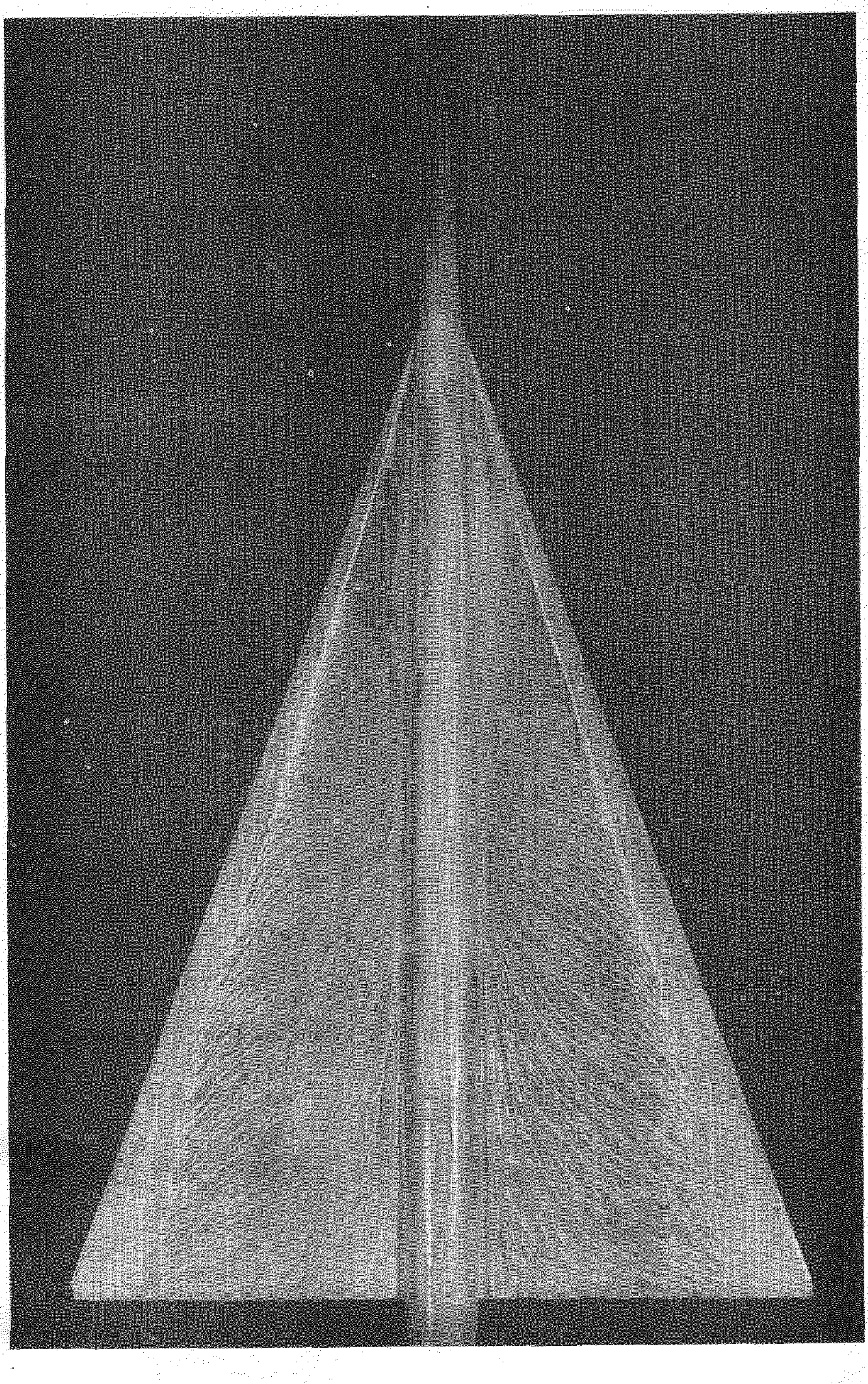

$\alpha = 34{\cdot}5^{0}$ $R = 0{\cdot}49 \times 10^{6}$

H.P. 100

Plate 7.

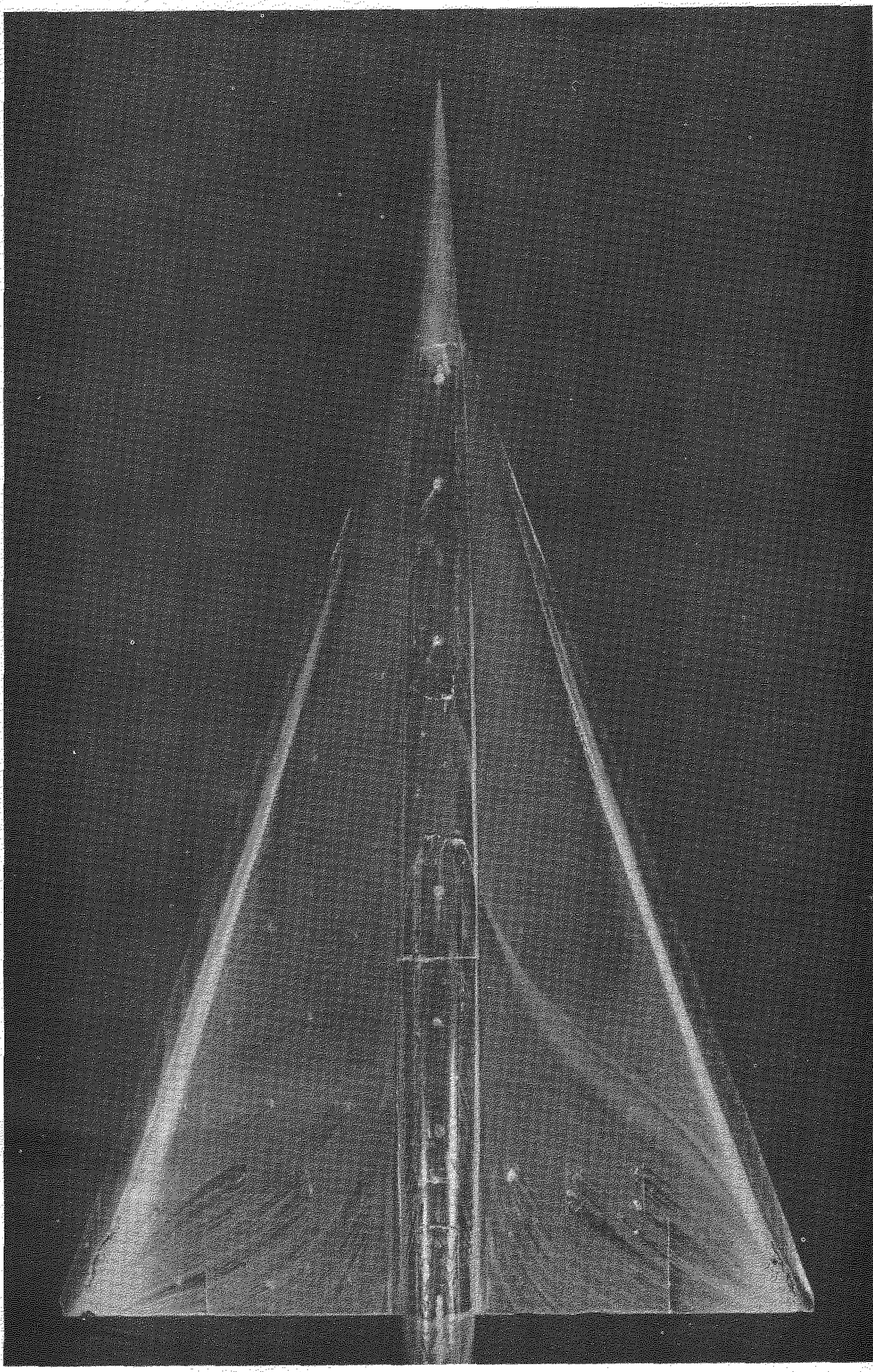

$\alpha = 34 \cdot 5^{\circ}$ $R = 5 \cdot 2 \times 10^{6}$

H.P. 100

DS 92699/1/WT52 K4 5/58 CL

C.P. No. 387
(18.084)
A.R.C. Technical Report

Printed and published by
HER MAJESTY'S STATIONERY OFFICE

To be purchased from
York House, Kingsway, London w.c.2
423 Oxford Street, London w.1
13A Castle Street, Edinburgh 2
109 St Mary Street, Cardiff
39 King Street, Manchester 2
Tower Lane, Bristol 1
2 Edmund Street, Birmingham 3
80 Chichester Street, Belfast
or through any bookseller

Printed in Great Britain

S.O Code No 23-9010-87

C.P. No. 387